Utilising measures of fiber dispersion in white matter tractography

Matthew Rowe, Hui Zhang, Daniel Alexander

Centre for Medical Image Computing, Department of Computer Science, University College London, UK
matthew.rowe.09@ucl.ac.uk

Abstract. This paper proposes a new tractography algorithm utilising measures of fiber dispersion derived from diffusion weighted magnetic resonance (DW-MR) imaging. Tractography estimates connectivity by integrating a pathway from a seed point following directional information derived from DW-MR images. Current tractography techniques follow a discrete set of directions given in each voxel of a DW-MR image and probabilistic techniques account for noise induced uncertainty on those discrete directions. Histological evidence suggests that fiber orientation dispersion exists in areas of white matter such as the centrum semiovale, representing a continuum of potential fiber orientations which cannot be accurately summarised by a limited set of discrete directions. Recent studies have shown that measures of fiber dispersion in brain white matter can be directly measured from DW-MR imaging data and explicitly represented in the orientation distribution function (ODF) of a voxel, but such measures have yet to be used in guiding tractography algorithms. We present a tracking algorithm which makes use of ODFs which account for underlying fiber dispersion to trace potential fiber pathways, we compare this method with traditional tracking methods on simulated data and *in vivo* human data, showing that measures of fiber dispersion can aid tractography in finding connectivity commonly missed by current tractography methods.

1 Introduction

Tractography is a powerful tool to probe the geometric structure of white matter non-invasively *in vivo* from diffusion weighted magnetic resonance images. Tractography algorithms estimate connectivity between different functional brain regions, giving us insight into brain function of great importance to neurological knowledge and understanding [1]. Tractography can also provide us with information on white matter structure which is difficult or impossible to define using anatomical images alone, aiding in surgical planning [2].

Tractography algorithms estimate connectivity by integrating pathways through a DW-MR image volume to estimate potential connections between different regions of the brain. Current deterministic and probabilistic tractography techniques follow a discrete set of directions given by diffusion tensor imaging [3]

or more sophisticated multifiber techniques such as Qball [4] and PASMRI [5], which account for multiple fiber populations per voxel. Probabilistic tractography accounts for noise-induced uncertainty in the dominant direction.

A significant flaw of current tractography approaches is the assumption of a discrete set of fiber directions per voxel. Post mortem dissection confirms that in addition to crossing fiber configurations, regions of fanning fibers exist in brain regions such as the centrum semiovale [6]. Current tractography techniques do not explicitly address the continuum of potential directions available in such regions due to underlying fiber dispersion.

Global tractography [7–9] provides an elegant solution to resolving contentious voxel fiber configurations such as crossing and fanning by solving for the entire projectome simultaneously. The drawback of a global approach is however the practicality of obtaining solutions. Many global tractography implementations require extensive computing resources or have long running times of several weeks on standard hardware. Combined with the fact that reaching the global minimum of such an astronomical optimisation is a practical impossibility, global tractography is not necessarily an ideal solution.

Recent studies [10–12] have demonstrated that intra-voxel fiber dispersion can be estimated using DW-MRI. These estimates of fiber dispersion within a voxel can provide tractography algorithms the appropriate basis to fully explore potential fiber pathways in regions of dispersing fiber structure such as the centrum semiovale, avoiding the potential for false negative connections due to the lack of coverage of the potential trajectories in fanning regions based on the assumption of discrete voxel fiber directions. Although Kaden *et al* [11] estimates fiber dispersion in each voxel this information is only used to sample the possible orientation at the initial tracking location, subsequent tracking is limited to following the principle direction in each incident voxel.

In this paper we present the first tracking algorithm utilising estimates of intra-voxel fiber dispersion to explore the connectome thoroughly. The algorithm makes use of distributions derived from fitting models intrinsically incorporating fiber dispersion to the diffusion weighted MR data using NODDI (neurite orientation dispersion and density imaging) [13]. Section 2.1 describes the method of obtaining the ODFs based on underlying fiber dispersion and in section 2.2 we outline the details of the tracking algorithm. In section 3.1 we present a comparison with traditional tracking methods on simulation data, showing the advantages of utilising dispersive ODFs. In section 3.4 we apply the algorithm to *in vivo* data and compare with results from traditional tracking.

2 Methods

2.1 DispersionODF

To obtain the dispersive ODFs from *in vivo* data we use NODDI [13], which produces estimates of the orientation distribution function (ODF). In [13] the ODFs are estimated by fitting a Watson distribution to the data. Here we extend the technique to account for cylindrically assymetrical dispersion by fitting

a Bingham distribution, the details of which will be reported elsewhere. The models are fitted to the data with the routine described in [14]. We find κ_1 and κ_2 for the Bingham model in every voxel where the Bingham distribution $f : \mathbb{S}^2 \mapsto \mathbb{R}^+$ is described as:

$$f(\mathbf{n}) = F_1\left(\frac{1}{2}, \frac{3}{2}, \kappa_1, \kappa_2\right)^{-1} \exp\left[\kappa_1(\boldsymbol{\mu}_1 \cdot \mathbf{n})^2 + \kappa_2(\boldsymbol{\mu}_2 \cdot \mathbf{n})^2\right] \tag{1}$$

κ_1 and κ_2 are parameters defining the degree of dispersion along the axes $\boldsymbol{\mu_1}$ and $\boldsymbol{\mu_2}$ respectively. $F_1(1/2, 3/2, \kappa_1, \kappa_2)$ is the hypergeometric function. A chosen fiber signal model is used to estimate the MR signal from a fiber orientation distribution described by the above Bingham distribution and κ_1, κ_2, $\boldsymbol{\mu_1}$ and $\boldsymbol{\mu_2}$ are optimised to find the best description for the data. An isotropic compartment is also added to the signal model. This provides us with a distribution representing fiber dispersion derived directly from a model fitted to the data in each voxel, representing an accurate estimate of the potential orientation dispersion of the underlying tissue.

The Bingham distribution is an antipodially symmetric distribution, which, in contrast to the Watson distribution, is not cylindrically symmetric, giving a measure of the degree of orientation dispersion separately for two orthogonal axes which are perpendicular to the principle direction. The Bingham distribution therefore nicely summarises the degree of fiber dispersion in each voxel along two seperate, orthogonal axes. Figure 1 shows Bingham distributions fitted in a voxel in the corpus callosum 1(a) and another voxel in the centrum semiovale 1(b) showing how the Bingham distribution captures the higher degree of dispersion in the centrum semiovale where histology confirms the presence of fanning fiber structures.

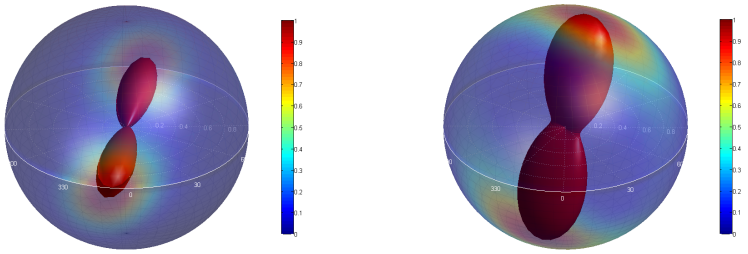

(a) (b)

Fig. 1. Example Bingham distributions fitted in single voxels in the mid-saggital corpus callosum 1(a) and deep within the centrum semiovale 1(b). The red interior structure shows the form of the distribution with probability density plotted with respect to polar radius. The probability density is also projected onto the translucent outer sphere in colour. The colour key depicts proportion of maximum probability density.

2.2 Tracking Algorithm

Our tracking algorithm adapts the strategy used by Friman in [15]. This approach allows us to employ a fully probabilistic framework exploring distributions based on fiber dispersion while applying suitable priors to limit curvature. Friman's approach accommodates only the uncertainty in the principle diffusion direction induced by noise, image artifacts and partial volume effects; we instead incorporate underlying fiber dispersion directly in the ODF used to guide the tracking.

Specifically, to propagate the track through the image, starting from a seed, we choose a propagation direction v_i from a distribution formed from the product of the local ODF and a prior on the allowable deviation from the previous direction v_{i-1}:

$$P(\hat{v}_i|\hat{v}_{i-1}, \kappa_1, \kappa_2) = \frac{P(\hat{v}_i|\kappa_1, \kappa_2)P(\hat{v}_i|\hat{v}_{i-1})}{P(\hat{v}_i)}\,, \tag{2}$$

where $P(\hat{v}_i|\kappa_1, \kappa_2)$ is the Bingham distribution described above.

For the angular Prior $P(\hat{v}_i|\hat{v}_{i-1})$, we use a distribution given by:

$$P(\hat{v}_i|\hat{v}_{i-1}) = \begin{cases} (\hat{v}_i^T \hat{v}_{i-1})^\gamma, & \text{if } \hat{v}_i^T \hat{v}_{i-1} \geq 0. \\ 0, & \text{if } \hat{v}_i^T \hat{v}_{i-1} < 0. \end{cases} \tag{3}$$

Sampling from this joint distribution allows exploration of the potential path directions in dispersive fiber regions while regularizing the curvature of the path. γ defines the strength of the curvature prior. Low values accommodate large degrees of deviation per track step, exploring more of the dispersion in each voxel, however, this also produces highly irregular tracts. Higher values promote smooth, slowly curving pathways which correspond to known tract geometries. Experiments on synthetic data suggest that a good choice for gamma is 24 (see section 3.2).

Due to the complexities and potential computational costs of various methods of sampling the continuous PDF given in equation 2 we choose, like Friman, to approximate the continuous PDF with a discrete PDF. By using a sufficiently large number of points spread evenly across the unit sphere and evaluating the PDF on the unit vector defined by each point and the origin, it is trivial to then draw a sample from this discrete PDF. As Friman, we use 2562 directions derived from the vertices on the unit sphere of a fourfold tesellation of an icosahedron.

3 Experiments and results

3.1 Synthetic experiments

For the experiments on synthetic data, we created a numerical phantom structure mimicking a region of dispersing fibers shown in Figure 2. The blue lines show a subset of the strands which form the structure to illustrate the geometry of the phantom. The region is 8 voxels wide by 6 voxels tall, with the voxel grid

shown behind the phantom. Each of the blue strands was subdivided into line segments of length much smaller than the voxel scale.

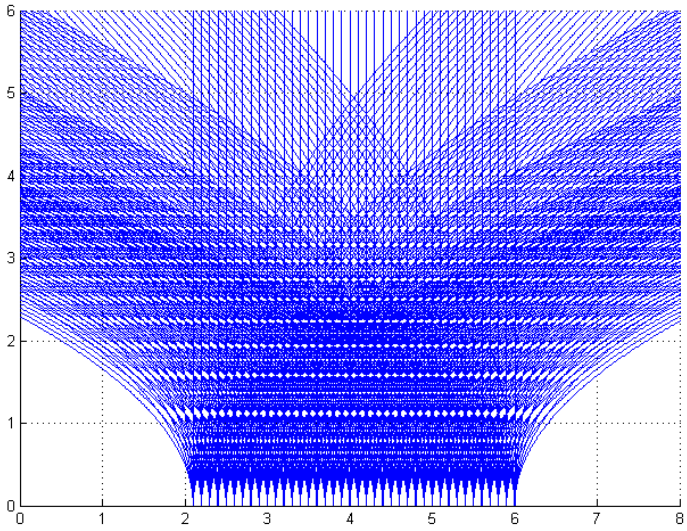

Fig. 2. Structure of synthetic dispersing phantom. The blue lines show a subset of the strands forming the structure, for illustration.

3.2 Determination of γ

We use the phantom described in section 3.1 to obtain the most appropriate value of γ. ODFs were derived by fitting Bingham distributions directly to the phantom structure in each voxel. We then tracked from a region of the base of the phantom using the algorithm described in section 2.2 with a range of values of γ (Figure 2). Figure 3(a) shows that at low values of γ such as 1, irregular tracks result, however, at a significantly higher value of $\gamma = 50$ (Figure 3(f)), such a strong prior on curvature can limit the potential trajectories of the tracks, hence limiting exploitation of the dispersive ODFs. Satisfactory results can be achieved for a range of intermediate values. For this demonstration of the algorithm we choose $\gamma = 24$ (Figure 3(e)), however, γ may reasonably be tuned within a range of values for other applications if necessary.

3.3 Tracking on synthetic data

To evaluate the effectiveness of utilising measures of underlying fiber dispersion in tractography, we created a simulated DW-MR dataset based on the phan-

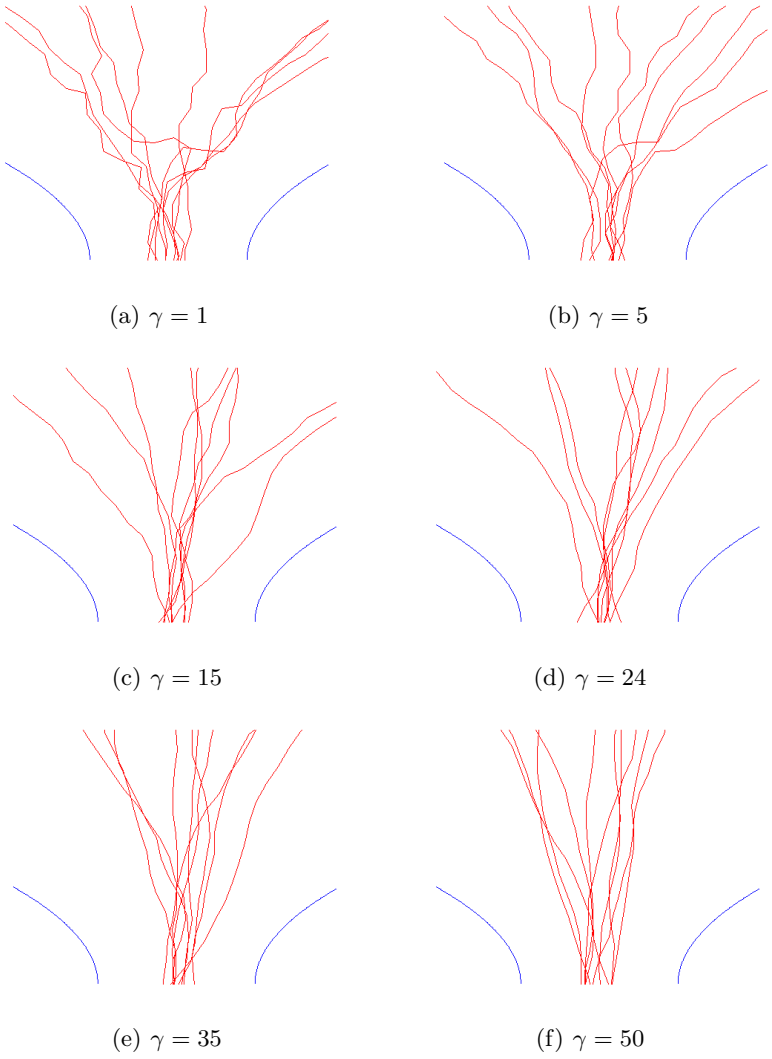

(a) $\gamma = 1$ (b) $\gamma = 5$

(c) $\gamma = 15$ (d) $\gamma = 24$

(e) $\gamma = 35$ (f) $\gamma = 50$

Fig. 3. Tracking through a synthetic region of dispersion utilising different values of the constant γ in equation 3. The blue lines represent the extremeties of the phantom described in section 3.1.

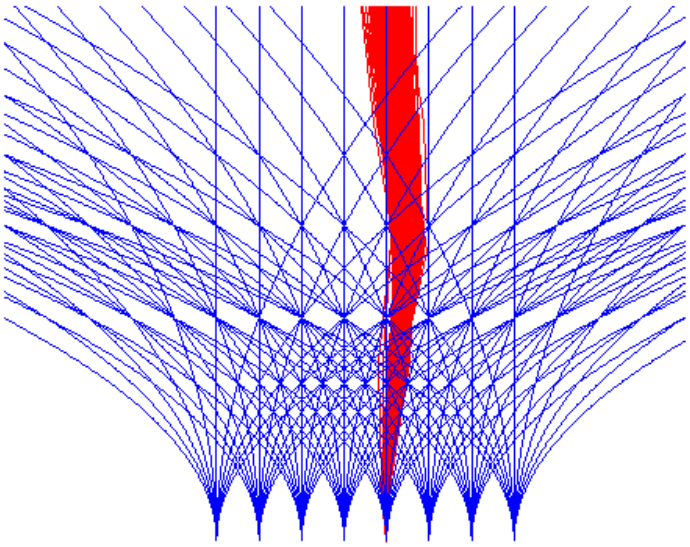

(a)

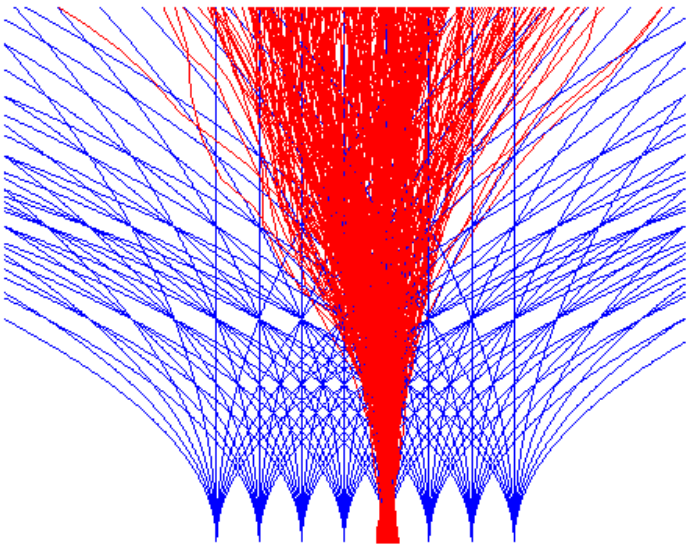

(b)

Fig. 4. Tractography based on standard PICo tractography techniques (Figure 4(a)) and using the tracking algorithm described in section 2.2 (Figure 4(b)). The Blue lines represent a sparse selection of the underlying fibers of the phantom described in section 3.1. The red lines represent the tracking result.

tom described above and tracked using traditional PICo tractography [16] for comparison. We then tracked using the algorithm described in section 2.2, using ODFs derived directly from the phantom structure. The DW-MR signal was simulated using a 30 direction gradient scheme [17] as the basis for a signal simulation using the diffusion tensor model. A diffusion tensor signal with $d_\perp = 3.5101\text{x}10^{-4}\text{mm}^2/\text{s}$ and $d_\parallel = 2\text{x}10^{-3}\text{mm}^2/\text{s}$ was simulated with a b-value of 1000 s/mm^2 for each line segment of the phantom and signals for all line segments residing in each voxel were summed and normalised. We then fit diffusion tensors to the artificial data derived from the phantom using the open source diffusion MRI toolkit Camino [18]. Bingham distributions were fit to the phantom fiber structure and used to track from a seed point at the base using the algorithm described in section 2.2 (Figure 4(b)). This is compared against standard PICo tracking (Figure 4(a)) using Camino.

3.4 *in vivo* data

We also test our tracking algorithm on *in vivo* data of a subject. DW-MR images of a healthy male were acquired on a clinical 3T Philips system with isotropic voxels of 2mm, TE=78ms, TR=12.5, with one 30 direction shell and one 60 direction shell with b-values of 1000 s/mm^2 and 2000 s/mm^2 respectively. This dataset is the same as that used in [13]. The Camino toolkit was then used to fit the diffusion tensor to the data and perform standard PICo tractography from a single voxel seed in the mid-saggital corpus callosum. Figure 3 demonstrates the performance of both standard PICo tractography (Figure 5(a)) and the algorithm presented in section 2.2 (Figure 5(b)) tracking from a seed voxel in the mid saggital corpus callosum. For both tracking examples, 5000 streamlines in total are propagated from a single seed voxel. Tracts are terminated upon entry into a grey matter mask extracted from a T1 weighted image using Freesurfer [19] which is then cooregistered to the diffusion weighted image.

3.5 Discussion

The experiments on simulated data detailed in section 3.1 show that tracking with traditional methods which ignore underlying fiber dispersion risks a large amount of false negative connections due to the limited exploration of the underlying fiber structure in regions exhibiting fiber dispersion. Figure 4(a) shows the algorithm presented in section 2.2 explores connectivity more thoroughly in such regions in this simple synthetic phantom. Figure 4 shows that including dispersion in tractography allows greater exploration of potential connectivity throughout the peripheral cortex. From a single voxel seed in the mid-saggital corpus callosum standard PICo tractography streamlines are directed vertically and do not explore the continuum of potential routes through the centrum semiovale (Figure 5(a)), whereas tractography based on the algorithm described in section 2.2 explores connectivity spread throughout the peripheral cortex (Figure 5(b)), the tract density is evenly spread through the intermediate region of

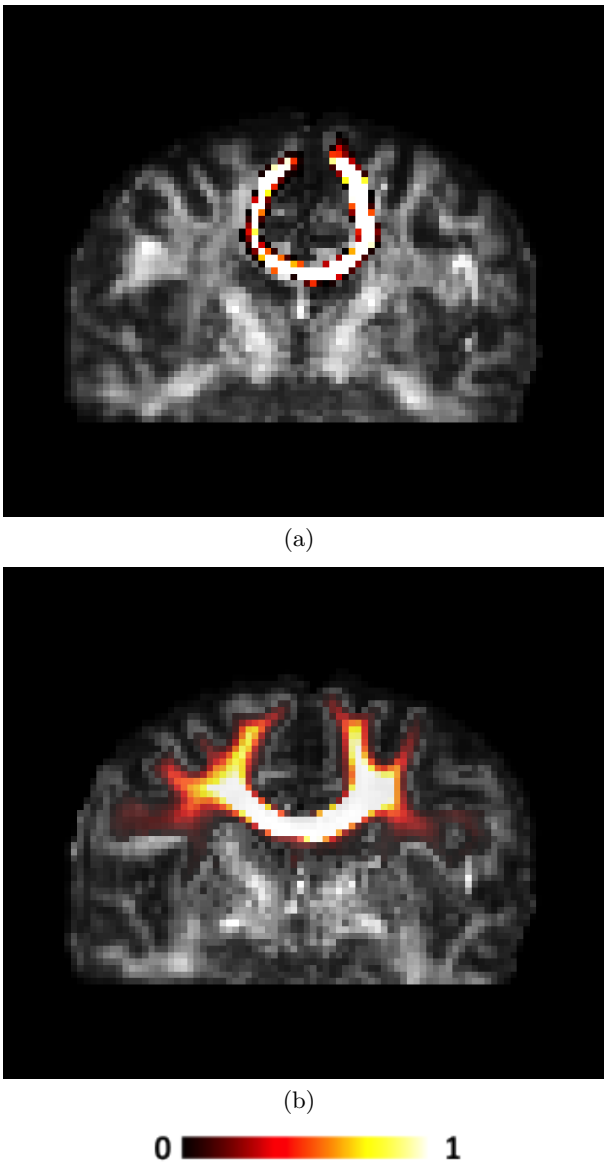

Fig. 5. Maximum intensity projection map of tractography based on standard pico tractography techniques (Figure 5(a)) and using the tracking algorithm described in section 2.2 (Figure 5(b)) overlayed on FA map.

the centrum semiovale, where histological study verifies there exists fanning fiber structure.

A problem that the algorithm does not currently address is that of fanning polarity. Local estimates of dispersion are symmetric, and hence don't distinguish the direction in which the fibers disperse. There is currently no known method to determine fanning polarity on the voxel scale [20], however recent work by Savadjiev [21] has made progress towards resolving the polarity of a fanning configuration by leveraging local voxel information. In future work, we plan to investigate the inclusion of such methods to further refine tractography including dispersion.

4 Conclusion

In this article, we present the first tracking algorithm (to our knowledge) utilising measures of intra-voxel fiber dispersion to explore the connectome. Including direct measures of intra-voxel fiber dispersion in tractography shows clear advantages in thoroughly exploring potential connections, exploring connectivity commonly missed by current tractography implementations.

References

1. Kasturi, N., Lichtman, J.W.: The rise of the 'projectome'. Nature Methods **4(4)** (2007) 307–308
2. Winston, G.P., Yogarajah, M., Symms, M.R., McEvoy, A.W., Micallef, C., Duncan, J.S.: Diffusion tensor imaging tractography to visualize the relationship of the optic radiation to epileptogenic lesions prior to neurosurgery. Epilepsia **52** (2011) 1430–1438
3. Basser, P.J., Mattiello, J., LeBihan, D.: MR Diffusion tensor spectroscopy and imaging. Biophys J. **66(1)** (1994) 259–267
4. Tuch, D.S.: Q-Ball Imaging. Magnetic Resonance in Medicine **52** (2004) 1358–1372
5. Jansons, K.M., Alexander, D.C.: Persistent angular structure: new insights from diffusion magnetic resonance imaging data. Inverse Problems **19** (2003) 1031–1046
6. House, E.I., Panksy, B.: A Functional Approach to Neuroanatomy. McGraw Hill (1960)
7. Kreher, B.W., Mader, I., Kiselev, V.G.: Gibbs Tracking: A Novel Approach for the Reconstruction of Neuronal Pathways. Magnetic Resonance in Medicine **60** (2008) 953–963
8. Fillard, P., Poupon, C., Mangin, J.F.: A Novel Global Tractography Algorithm Based on an Adaptive Spin Glass Model. MICCAI **60** (2009) 927–934
9. Sherbondy, A.J., Dougherty, R.F., Ananthanarayanan, R., Modha, D.S., Wandell, B.A.: Think Global, Act Local; Projectome Estimation with Bluematter. MICCAI (2009) 861–868
10. Zhang, H., Hubbard, P.L., Parker, G.J.M., Alexander, D.C.: Axon diameter mapping in the presence of orientation dispersion with diffusion MRI. NeuroImage **56** (2011) 1301–1315
11. Kaden, E., Knosche, T.R., Anwander, A.: Parametric spherical deconvolution: Inferring anatomical connectivity using diffusion MR imaging. NeuroImage **37** (2007) 474–488

12. Sotiropoulos, S.N., Behrens, T.E.J., Jbabdi, S.: Ball and rackets: Inferring fiber fanning from diffusion-weighted MRI. NeuroImage **60** (2012) 1412–1425
13. Zhang, H., Shneider, T., Wheeler-Kingshott, C., Alexander, D.C.: NODDI: Practical in vivo neurite orientation dispersion and density imaging of the human brain. NeuroImage **61** (2012) 1000–1016
14. Alexander, D.C., Hubbard, P.I., Hall, M.G., Moore, E.A., Ptito, M., Parker, G.J.M., Dyrby, T.B.: Orientationally invariant indices of axon diameter and density from diffusion MRI. Neuroimage **52(4)** (2010) 1374–1389
15. Friman, O., Farneback, G., Westin, C.F.: A Bayesian Approach for Stochastic White Matter Tractography. Transactions on Medical Imaging **25(8)** (2006) 965–978
16. Parker, J.M., Haroon, H.A., Wheeler-Kingshott, C.A.M.: A Framework for a Streamline-Based Probabilistic Index of Connectivity (PICo) Using a Structural Interpretation of MRI Diffusion Measurements. Journal of Magnetic Resonance Imaging **18** (2003) 242–254
17. Jones, D.K., Horsfield, M.A., Simmons, A.: Optimal strategies for measuring diffusion in anisotropic systems by MRI. Magnetic Resonance in Medicine **42(3)** (1999) 515–525
18. Cook, P.A., Bai, Y., Nedjati-Gilani, S., Seunarine, K.K., Hall, M.G., Parker, G.J., Alexander, D.C.: Camino: Open-Source Diffusion-MRI Reconstruction and Processing. ISMRM (2006) 2759
19. Freesurfer: http://surfer.nmr.mgh.harvard.edu/
20. Jbabdi, S., Johansen-Berg, H.: Tractography: Where do we go from here? Brain Connectivity **1(3)** (2011) In Press
21. Savadjiev, P., Cambell, J.S.W., Descoteaux, M., Deriche, R., Pike, G.B., Siddiqi, K.: Labeling of ambiguous subvoxel fibre bundle configurations in high angular resolution diffusion MRI. NeuroImage **41** (2008) 58–68